Mechanistic details on Pd(II)/5,10,15,20-tetrakis(1-methyl-4-pyridiyl)-porphyne complex formation and reactivity in the presence of DNA

Tarita Biver[1] ● Sabriye Aydinoglu[2] ● Daniele Greco[1] ● Francesca Macii[1]

Received: ……/Accepted …

Abstract Kinetics of coordination of Pd(II) by the macrocyclic porphyrin 5,10,15,20-tetrakis(1-methyl-4-pyridiyl)-porphyne (H_2P^{4+}) is investigated and confirms quantitative formation of a planar PdP^{4+} complex at room temperature (formation rate 0.19 $M^{-1}s^{-1}$ at 25°C, 0.2M NaCl, pH 3). Then, the binding ability to DNA of the pre-formed PdP^{4+} complex is analysed. To this aim spectrophotometry, spectrofluorometry and viscometry are used. Thermodynamic parameters for binding, obtained by the temperature dependence of the equilibrium constants, are ΔH = -17 kcal mol^{-1} and ΔS = -32 cal mol^{-1} K^{-1}. These values, being both highly negative, agree with full PdP^{4+} intercalation into DNA. Moreover, kinetics of the binding reaction is analysed by the T-jump technique (reaction times in the 1-5 ms range). Experiments on the porphyrin ligand retention on negative SDS and positive DTAC micellar surfaces are also done. Taken altogether, these data provide mechanistic details on complex formation and on DNA

binding and relevant energies and driving forces. It is found that interaction between PdP^{4+} and base pairs is very strong (K^{DNA}_{abs} = 8.0×10^5 M^{-1} at 25°C, 1.0 M NaCl), not only owing to the high positive charge borne by the complex, but also to the contribution of high hydrophobicity of the porphyrin ring. In the dye/DNA complex, PdP^{4+} is buried into the helix, as confirmed also by fluorescence quenching tests. Both presence and type of metal ion play a major role, as lower affinity and lower induced helix conformation changes are found in the case of the H_2P^{4+}/DNA and CuP^{4+}/DNA systems.

Keywords Intercalation compounds ● Kinetics ● Reaction mechanisms ● Fluorescence Spectroscopy ● Micelles ● Nucleic acids

✉ Tarita Biver
Tarita.biver@unipi.it

[1] Department of Chemistry and Industrial Chemistry, University of Pisa, Pisa, Italy

[2] Department of Analytical Chemistry, Faculty of Pharmacy, Cukurova University, Adana, Turkey

Introduction

Metal complexes of porphyrins are known and used since long time; however, the interest in this family of molecules is still high. This is due to possible applications in frontier technologies as, for instance, anticancer drugs and G-quadruplexes stabilizers [1,2], active species in photodynamic therapy (PDT) [3,4], or as new materials for carbon nanotubes-based sensors/catalysts [5-7] and dye sensitized solar-cells [8,9].

Pd(II)-porphyrin complexes can be used as catalysts [10], for instance in the Suzuki-Miyaura reaction in water solvents [11]. Moreover, as for the biochemical aspects, palladium complexes are analysed as alternative of the known platinum ones [12,13]. Interestingly, Pd(II)-porphyrins were shown to bind DNA producing growth inhibitory effects [14,15].

After the pioneering work of Pasternack and collaborators [16-18], studies on porphyrin metal complexes often focused on the analysis of equilibria and overall properties [19]. Among them, palladium complexes have been less analysed respect to other metal ions [20-23] and kinetic studies on Pd-porphyrin complexes are relatively rare [24]. The Pd(II)-porphyrin complexes are often synthesized via relatively complex procedures [21,22]. Metallo-porphyrins are known to intercalate between DNA base pairs, but the exact nature of the interaction and extent of

insertion can be tuned by the presence axial ligands or sitting-atop geometries [18].

The aim of the here presented data, also making use of a kinetic approach, is to collect mechanistic details on the process of palladium-porphyrin complex formation in water by simple reactants mixing and on the reactivity of the formed complex towards biological substrates. The here analysed work focuses, as the ligand, on the water soluble, positively charged meso-tetrakis(l-methylpyridinium-4-yl) porphyrin (Figure 1) and mainly on the $PdCl_4^{2-}$ species (which will be majority under non strongly acidic pH conditions and in the presence of chloride ions [25]).

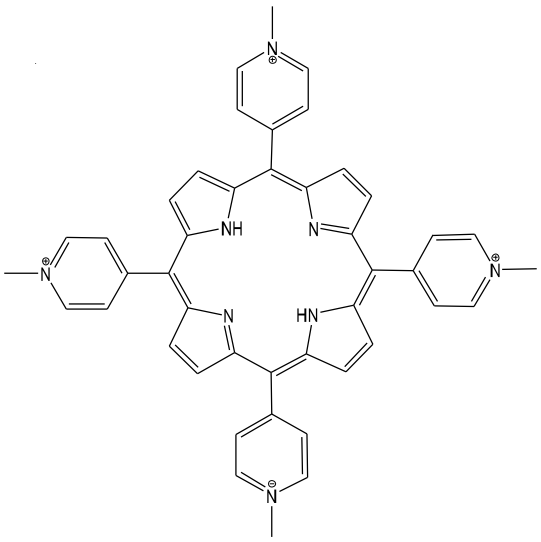

Fig. 1. Molecular formula of 5,10,15,20-tetrakis(1-methyl-4-pyridiyl)-porphyne in its unprotonated form (H_2P^{4+}).

Results and Discussion

Pd-porphyrin complex formation

The UV-vis spectrum of free porphyrin (H_2P^{4+}) changes upon metal ion complexation as reported in Figure 2A. Some peak widening indicates auto-aggregation of the metal complex. The non-dramatic bathochromic shift observed upon binding (λ_{max} from 423 nm to 434 nm) is in agreement with the formation of a complex where palladium is coordinated in its typical square planar geometry in the porphyrin plane [3]. In fact, out of plane geometries for the metal ion yield different typical signatures [4]. Under the experimental conditions used (pH 3.0, NaCl 0.2 M), palladium will be predominantly in the $PdCl_4^{2-}$ form [5]. The presence of NaCl is connected to physiological conditions and ensures Pd(II) stabilisation [5]. Figure 2B shows absorbance variation in time (differential spectra, i.e. equal palladium added in the reference cell) used to monitor complex formation kinetics.

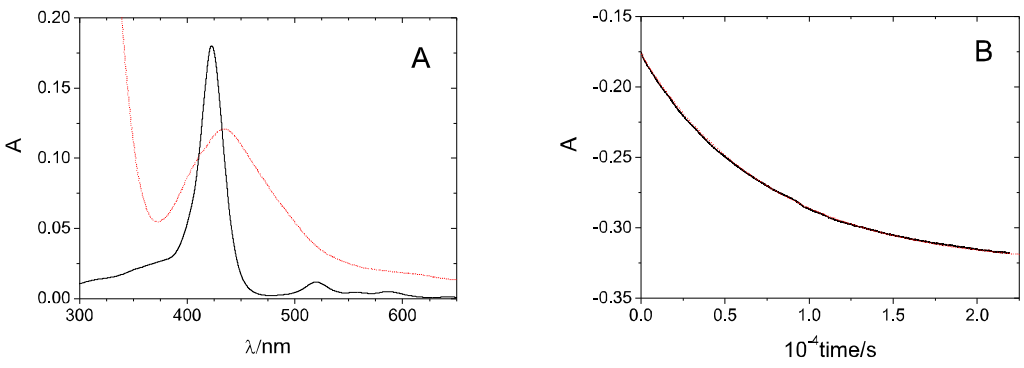

Fig. 2. A) UV-vis spectra in water of 9.6×10^{-7} M H_2P^{4+} (▬) and of 9.6×10^{-7} M H_2P^{4+} + 7.05×10^{-4} M $PdCl_4^{2-}$ (- • -); B) absorbance difference (see Methods section) variation in time at λ = 422 nm that monitors PdP^{4+} complex formation for 9.6×10^{-7} M H_2P^{4+} + 7.05×10^{-4} M $PdCl_4^{2-}$, the dotted line is the mono-exponential fit. For both A) and B) $[H^+] = 10^{-3}$ M, I = 0.2 M (NaCl), T = 25°C.

A series of experiments was performed by keeping the porphyrin (ligand, L) content constant and varying the palladium (metal, M) concentration under conditions of metal excess ($C_M >> C_L$). These experiments were repeated at different temperatures (25, 40, 55 and 65°C). The curves were mono-exponential. The relevant calculated time constant, $1/\tau$, depends on the metal content as reported in Figure 3. Note that the intercept is non distinguishable from zero at 25°C and 40°C. This indicates that a quantitative reaction is taking place under these relatively low temperature conditions, whereas the process becomes non-quantitative by increasing temperature.

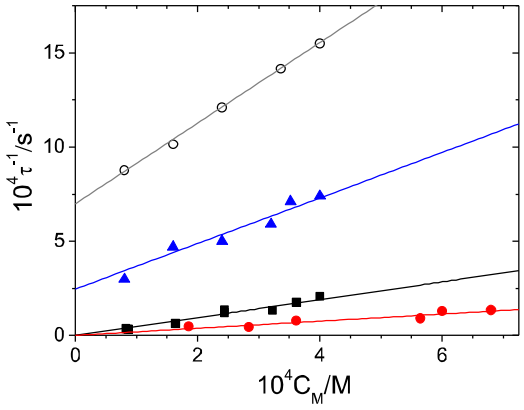

Fig. 3. Time constant ($1/\tau$) dependence on the palladium content ($C_M >> C_L$) for the formation of PdP^{4+} metal complex; $C_L = 9.6\times10^{-7}$ M, $[H^+] = 10^{-3}$ M, I = 0.2 M (NaCl), T = 25 °C (●), 40 °C (■), 55 °C (▲) and 65 °C (○).

The binding reaction can be written as the following apparent reaction (Eq. (1)).

$$H_2P^{4+} + Pd_f \underset{k_d^{app}}{\overset{k_f^{app}}{\rightleftharpoons}} PdP^{4+} + 2H^+ + nCl^- \qquad (1)$$

where Pd_f is the overall content of free metal ion that takes into account both $PdCl_4^{2-}$ and some limited amount of both $Pd(H_2O)Cl_3^-$ species (that will be largely minority under our conditions [5] but much more reactive) and aggregates. Taking into account that experiments are carried out at constant H^+ and Cl^-, the equilibrium constant relevant to Eq. (1) can be written as $K_{app} = [PdP^{4+}]/[Pd_f][H_2P^{4+}]$. Under the circumstances of high

metal excess respect to ligand, for the total metal ion concentration C_M = Pd_f + PdP^{4+} ≈ Pd_f holds and the following equation for the time constant applies (Eq. (2))

$$\frac{1}{\tau} = k_f^{app} C_M + k_d^{app} \quad (2)$$

Figure 3 shows the linear fits of the data according to the above relationship and Table 1 collects the values obtained for the relevant kinetic parameters.

Table 1. Apparent kinetic parameters for PdP^{4+} complex formation; I = 0.2 M (NaCl), pH = 3. *Data in italics* are rough estimates, based on the non-distinguishable from zero intercepts of the plots in Figure 3.

T **/°C**	25	40	55	65
$\mathbf{k_f^{app}}$ **/M^{-1} s^{-1}**	0.19	0.47	1.21	2.14
$\mathbf{k_d^{app}}$ **/s^{-1}**	*< 2.0×10^{-6}*	*< 1.0×10^{-5}*	2.46×10^{-4}	6.99×10^{-4}
$\mathbf{K_{app}}$ **/M^{-1}** [a]	*> 9.5×10^{4}*	*> 4.7×10^{4}*	4.92×10^{3}	3.06×10^{3}

[a] $K_{app} = k_f^{app}/k_d^{app}$

The k_f^{app} values are low, in agreement with the energy barrier penalty to be overcome for both the rigidity of the ring and H^+ and Cl^- expulsion consequent to formation of the PdP^{4+} complex. The analysis of the

dependence of k_f^{app} on temperature using the Eyring equation (Figure S1 of the Electronic Supplementary Material) yields $\Delta G^{\ddagger}_{app}$ = 18.5 Kcal mol^{-1}, $\Delta H^{\ddagger}_{app}$ = 12.7 Kcal mol^{-1} and $\Delta S^{\ddagger}_{app}$ = -19.3 cal mol^{-1} K^{-1} for respectively the activation free energy, enthalpy and entropy related to the formation of PdP^{4+}. The $\Delta S^{\ddagger} < 0$ value agrees with the associative inner sphere complexation mechanism typical of the Pd^{2+} ion [6,7].

Figure 4 shows the result of kinetic experiments, where the time constant $1/\tau$ is measured (at constant H_2P^{4+} and $PdCl_4^{2-}$) as a function of the medium. Full circles are the experiments at different [NaCl] (different ionic strength and thus different shielding effect), whereas open squares refer to experiments at different [NaCl] but [NaCl]+[$NaClO_4$] = constant = 0.2 M (i.e. constant ionic strength, i.e. constant shielding effect). Under the explored circumstances the reaction quantitative and, thus, $k_d^{app} = 0$. Accordingly, the relationship $1/\tau = k_f^{app} C_M$ holds (Eq. (2)). This means that, in Figure 4, changes in the measured reaction time, $1/\tau$, are proportional to changes in the value of the forward rate constant, k_f^{app}.

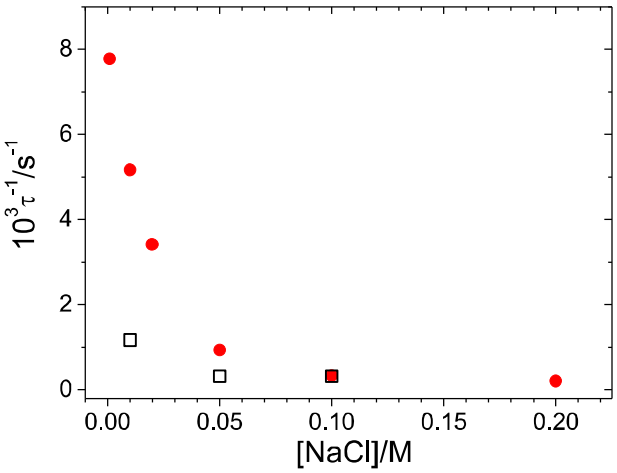

Fig. 4. Time constant ($1/\tau$) dependence on the medium for the formation of PdP^{4+} metal complex; $C_L = 9.6\times10^{-7}$ M, $C_M = 4.0\times10^{-4}$ M, $[H^+] = 10^{-3}$ M, *T* = 40 °C; (●) different [NaCl] and thus different total salt content; (■) experiments at I = 0.2 M = [NaCl] + [$NaClO_4$].

The circles show that the [NaCl] decrease produces significant increase of the reaction rates. This can be due either to the lower total ionic strength (I) of the medium (in agreement with the high, opposite, charge borne by the reaction partners) or to the borne of aquo-Pd-species. In experiments at constant I (open squares), this increase is quite totally cancelled, demonstrating that the shielding effect plays a major role. However, the value at [NaCl] = 0.01 M still shows a kinetic increase: under low chloride conditions, $PdCl_4^{2-}$ is likely to become minority in favour of the $Pd(H_2O)Cl_3^-$ species [5]. The latter reacts much faster than $PdCl_4^{2-}$; in

fact, the energy barrier is lower in the case of $Pd(H_2O)Cl_3^-$ due to the increased lability of the Pd-H_2O bond in comparison with the Pd-Cl bond. On the whole, a reaction mechanism that considers $Pd(H_2O)Cl_3^-$ as the main reacting species can be proposed, as shown below (Eq. (3)).

$$H_2P^{4+} + Pd(H_2O)Cl_3^- \rightleftharpoons PdP^{4+} + 2H^+ + 3Cl^- \quad (3)$$

$$\uparrow\downarrow +Cl^-$$

$$PdCl_4^{2-}$$

The reaction mechanism above enlightens the practical point that, being PdP^{4+} quantitatively formed in the presence of a relatively concentrated NaCl buffer (our study), this ensures that it will even better be formed in the presence of Pd(II) aquo-species, as far as problems due to formation of hydroxo-species are avoided.

Pd-porphyrin complex interaction with DNA

Absorbance and fluorescence titrations For these studies the PdP^{4+} complex (dye, D) was pre-formed by mixing equimolar quantities of the reagents under conditions of quantitative reaction (25 or 40°C). Its overall analytical molar concentration is from now on indicated as C_D. Figure 5A shows the data recorded during a spectrophotometric titration where increasing amounts of DNA (polynucleotide, its overall analytical molar

concentration in base pairs is from now on indicated as C_P) were added to the cell containing the PdP^{4+} complex. The DNA experiments where done at relatively high salt content (NaCl 1.0 M) as, at lower ionic strength, the binding turned to be quantitative (not shown). Note that the effect of the ionic strength is swamped off (Figure 4), so that the reaction between metal and ligand will be quantitative at I = 1.0 M as well. Hypochromic and bathochromic effects suggest an intercalative binding mode, even if the non-perfect isosbestic point indicates non-simple binding (see comments below on dye aggregation on the DNA surface). Figure 5B shows the relevant binding isotherm at 417 nm, where $\Delta A = A - A_0$ and A_0 is the absorbance in the absence of DNA.

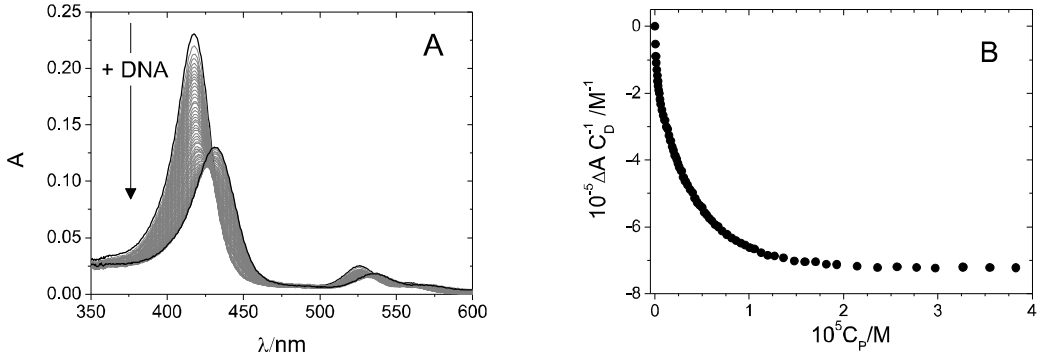

Fig. 5. (A) PdP^{4+} absorbance spectra variation upon addition of increasing amounts of DNA and (B) relevant binding isotherm at 417 nm; C_D = 2.0 μM, C_P = 0 to 38 μM, pH 7.0, NaCl 1.0 M, NaCac 0.01 M, T = 25.0°C.

The interaction between a DNA reacting site (base pair, P) and the porphyrin dye (D) to give the complex (PD) can be described by a simplified 1:1 reaction model (reaction (4))

$$P + D \leftrightarrows PD \quad (4)$$

The evaluation of the binding constant for reaction (4), K^{DNA}, can be done by analysing the spectrophotometric data using Eq. (5)

$$\frac{C_P C_D}{\Delta A} + \frac{\Delta A}{\Delta \varepsilon^2} = \frac{1}{K^{DNA} \Delta \varepsilon} + \frac{1}{\Delta \varepsilon}(C_P + C_D) \quad (5)$$

where C_P and C_D are the total analytical dye and DNA concentrations respectively and $\Delta\varepsilon = \varepsilon_{PD} - \varepsilon_D$ is the variation of the optical parameters upon binding. According to Eq. (5), a plot of $C_P C_D/\Delta A + \Delta A/\Delta\varepsilon^2$ vs. (C_P + C_D) should yield a straight line with $\Delta\varepsilon$ = 1/slope and K^{DNA} = slope/intercept. An iterative procedure is needed as $\Delta\varepsilon$ is not known: in a first approximation $\Delta A/\Delta\varepsilon^2 = 0$ so to obtain a first $\Delta\varepsilon$ evaluation from reciprocal slope, this is used to replot the data and so on until convergence is reached. Figure S2 shows an example of data analysis; at 25°C K^{DNA} (absorbance) = $(8.0\pm0.3)\times10^5$ M^{-1}. Spectrophotometric titrations were repeated at different temperatures (ranging from 15°C to 40°C), Figure 6 shows a vant'Hoff plot of the results.

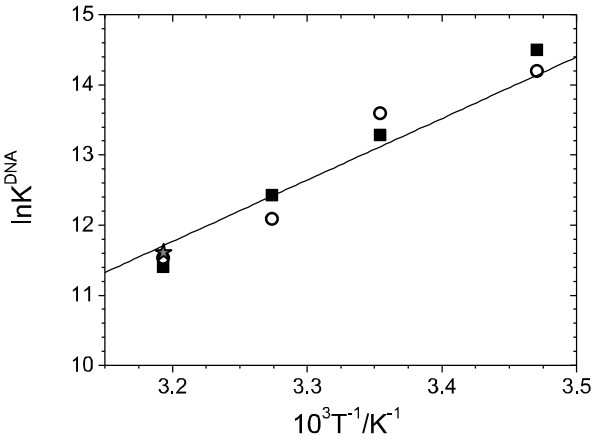

Fig. 6. Van't hoff plot for the PdP^{4+}/DNA system; ■ spectrophotometric titrations, ○ spectrofluorometric titrations, ★ kinetics ($K^{DNA} = k_f^{DNA}/k_d^{DNA}$), pH 7.0, NaCl 1.0 M, NaCac 0.01 M.

The titrations were repeated using fluorescence detection. The intensity of the emission spectrum of PdP^{4+} decreases upon DNA addition (Figure S3) and the relevant binding isotherm is obtained (Figure 7). This is analysed according to Eq. (5) simply replacing ΔA by $\Delta F = F - \varphi_D C_D$ and $\Delta\varepsilon$ by $\Delta\varphi = \varphi_{PD} - \varphi_{D,}$ the change in the optical parameters (inset of Figure 7). At 25°C K^{DNA} (fluorescence) = $(6.3\pm0.3)\times10^5$ M^{-1}, in good agreement with previous findings. Binding constant values obtained from fluorescence titrations at different temperature are also shown in Figure 6. On the whole, assuming the ΔH and ΔS are constant over the reduced temperature range

studied, it turns out that ΔH = -17 kcal mol^{-1} and ΔS = -32 cal mol^{-1} K^{-1}. These values, being both highly negative, agree with the common signature of an intercalative binding mode [8].

For both absorbance and fluorescence data (collected at similar dye concentrations) the very first experimental points could be found to deviate from the theoretical linear trend under conditions of high dye excess (beginning of titration). Dye dimerization will be repressed under these relatively high salt content conditions but some DNA induced aggregation on the polynucleotide surface can occur for $C_D >> C_P$: the relevant data point were disregarded in the above described data analysis.

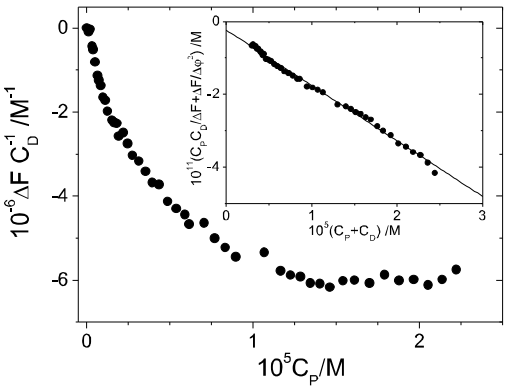

Fig. 7. Binding isotherm for PdP^{4+}/DNA fluorescence titration and relevant analysis according to Eq. (5) (inset); C_D = 2.5 μM, C_P = 0 to 22 μM, λ_{ex} = 500 nm, λ_{em} = 572 nm, pH 7.0, NaCl 1.0 M, NaCac 0.01 M, T = 25.0°C.

Kinetics The kinetic analysis of PdP^{4+} binding to DNA was done using the T-jump technique at 40°C, at 25 °C the signal/noise ratio was too unfavourable. Figure 8A shows an example of the mono-exponential relaxation curves registered, whereas Figure 8B is a plot of the reciprocal time constant, $1/\tau$, calculated from data fit, as a function of reactants concentrations.

Eq. (6) do apply, where [P]+[D], the sum of the reactants in the free form at equilibrium, is first calculated using the K^{DNA} value from absorbance, then iteratively from $K^{DNA} = k_f^{DNA}/k_d^{DNA}$ until convergence is reached. It turns out that $k_f^{DNA} = (1.7\pm0.1)\times10^7$ $M^{-1}s^{-1}$, $k_d^{DNA} = (1.6\pm0.2)\times10^2$ s^{-1} and $K^{DNA} = k_f^{DNA}/k_d^{DNA} = (1.1\pm0.2)\times10^5$ $M^{-1}s^{-1}$ in very good agreement with our previous thermodynamic findings (Figure 6).

$$\frac{1}{\tau} = k_f^{DNA}([P]+[D]) + k_d^{DNA} \qquad (6)$$

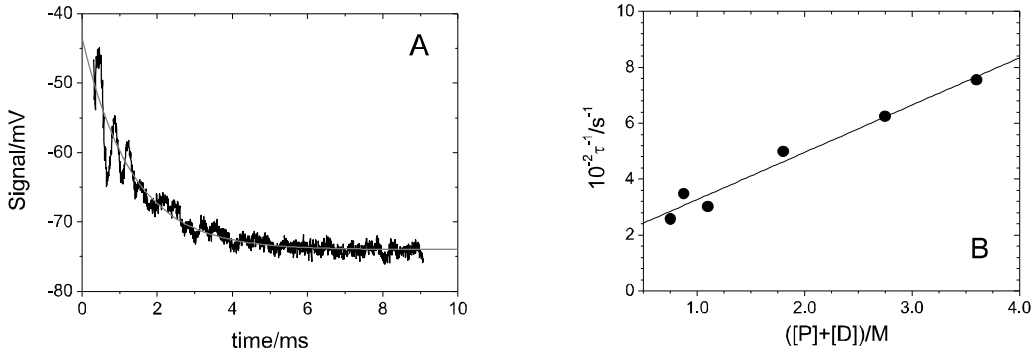

Fig. 8. Kinetic analysis (T-jump technique) of PdP^{4+}/DNA binding: A) example of relaxation curve (C_P = 38.7 μM, λ = 420 nm) and B) reciprocal relaxation time dependence on reactant concentrations (C_P = 5.0 to 38.7 μM); C_D = 2.0 μM, pH 7.0, NaCl 1.0 M, NaCac 0.01 M, T = 40.0°C.

The k_f value is significantly high, near to diffusion limit and orders of magnitude higher than that found for DNA intercalation of other aromatic macrocyclic metal-complexes [9,10]. This result can be ascribed both to the high charge borne by PdP^{4+} and to its planarity, which enables dye insertion between the base pairs without high energy barriers to be overcome for penetration.

Fluorescence quenching Stern-Volmer plots for quenching by the iodide ion of the PdP^{4+} complex and PdP^{4+}/DNA mixture are shown in Figure 9. Cancellation of any quenching effect in the presence of DNA confirms strong penetration of the porphyrin complex into the nucleotide helix, in agreement with a model that considers full intercalation of the planar complex. A similar effect is not obtained for H_2P^{4+}, where some quenching does occur also in the presence of DNA (Figure S4). This result indicates significant influence of the presence of the palladium ion in the binding mode.

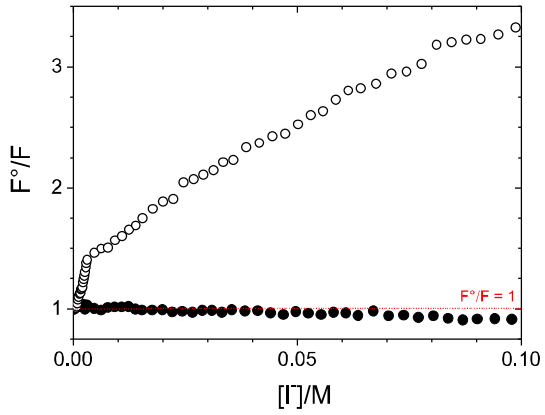

Fig. 9. Stern-Volmer plot for the quenching by iodide of PdP^{4+} (open mark) and PdP^{4+}/DNA (full mark); C_D = 1.9 μM, C_P = 24.9 μM, λ_{ex} = 470 nm, λ_{em} = 555 nm, pH 7.0, T = 25.0°C.

Viscosity The relative viscosity η/η° of the PdP^{4+}/DNA system changes as a function of the C_D/C_P ratio (Figure 10), where

$$\frac{\eta}{\eta^\circ} = \frac{t - t_{solv}}{t_{DNA} - t_{solv}} \qquad (7)$$

and t, t_{solv} and t_{DNA} denote respectively the flow time of the sample (PdP^{4+}/DNA mixture), of the solvent (0.1 M NaCl, 0.01 M NaCac) and of solvent + DNA 2.8×10^{-4} M. Here, the salt content is low to favour quantitative binding. The results clearly confirm that PdP^{4+} strongly interacts with DNA, with important changes of the relative viscosity that

can be connected to intercalative binding. In agreement with quenching experiments, viscosity data confirm that the absence of palladium turns into weaker interaction (see significantly reduced changes in case of H_2P^{4+}). The type of metal ion also plays a role: the CuP^{4+} complex is not able to alter DNA conformation as much as PdP^{4+}.

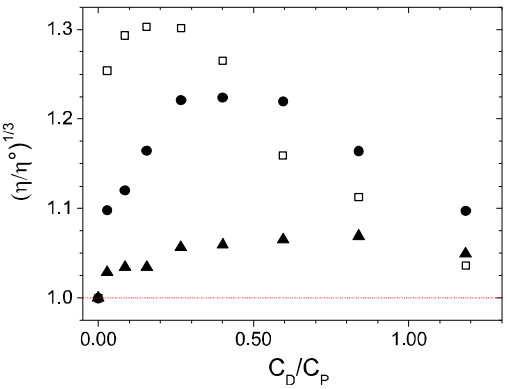

Fig. 10. Relative viscosity $(\eta/\eta°)^{1/3}$ dependence on the dye/DNA ratio for different porphyrin/DNA systems: (□) PdP^{4+}, (●) CuP^{4+} (▲) and H_2P^{4+}; C_P = 2.79×10^{-4} M, NaCl 0.1 M, pH 7.0, T = 25.0°C.

Slow kinetic effect Difference spectra (PdP^{4+} vs. PdP^{4+}/DNA) where registered in time (Figure S5) that showed that the recorded signal changes in the dozen of minutes time range. Figure 11 reports the percentage of absorbance variation (100*|A(t)-A(0)|/A(0)) in time at different wavelengths. A metal ion can, according to slow kinetics [11],

covalently bind to the nucleobases [12,13]. The trend observed is consistent with a slow kinetic attack of Pd(II) to the DNA bases and/or with a slow rearrangement of the DNA backbone to better accommodate the intercalator. This process can account for the stronger effect on the DNA conformation shown by PdP^{4+} respect to H_2P^{4+} and CuP^{4+} (Figure 10).

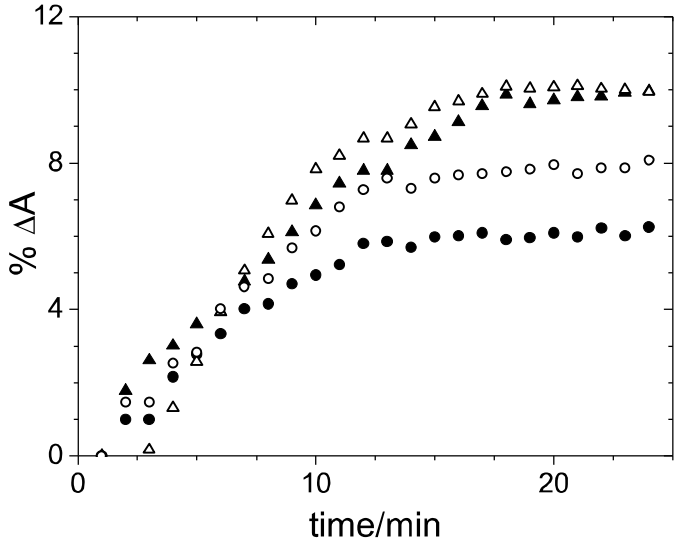

Fig. 11. Percentage of absorbance variation (100*|A(t)-A(0)|/A(0)) in time for the PdP^{4+}/DNA system at different wavelengths; $C_D = 1.77\times10^{-5}$ M, $C_P = 1.81\times10^{-4}$ M, I = 1.0 M, pH = 7.0, T = 25.0 °C, total time = 186 min; (Δ) 415 nm, (▲) 439 nm, (○) 522 nm, (●) 542 nm.

Micellar media To enlighten some aspects of DNA binding, the characteristics of the porphyrin ligand and its PdP^{4+} complex were better analysed by experiments in micellar media. It was observed that H_2P^{4+}

protonation becomes very difficult in sodium dodecyl sulphate (SDS) micellar media (Figure S6A). UV-vis acid titrations show that in SDS, even at pH = 0.47, only partial formation of the H_3P^{5+} species is achieved (Figure S6B), whereas in water biprotonation with pK_{A1} = 1.0 and pK_{A2} = 2.5 are found (Figure S7), in agreement with literature [14,15]. For other dyes, the pK_A values are found to increase in the presence of anionic micelles due to H^+ concentration at the negative micellar surface and relevant surface potential modification [16]. For the here analysed system the opposite occurs. Given that [SDS] >> [porphyrin] so that the surface potential is not supposed to change much due to H_2P^{4+}, the explanation is to be found in the very high hydrophobicity of the ligand that tends to be buried inside the micellar core, far away from outer reactants. Accordingly, the absorption maximum of H_2P^{4+} shifts from 422 nm in water to 426 nm in SDS, indicating strong interaction and polarity changes. Moreover, ultrafiltration experiments indicate that 94% of the ligand is retained on the SDS surface ([SDS] = 0.03M, no NaCl added, based on spectrophotometric data before and after ultrafiltration, λ = 426 nm, 25°C) and that 22% of the ligand is retained on the positive dodecyl trimethyl ammonium chloride (DTAC) surface ([DTAC] = 0.03M, no NaCl added, based of spectrophotometric data before and after ultrafiltration, λ = 426 nm, 25°C). The latter result confirms the very high hydrophobicity of the H_2P^{4+} ligand,

a driving force able to overcome the repulsion towards the positive DTAC micelle. Looking at the complexation reaction in SDS, no interaction between H_2P^{4+} and palladium ion seems to be possible at pH 2.0 and NaCl 0.11M or 0.01M ($PdCl_4^{2-}$ and $Pd(H_2O)Cl_3^-$ species majority [5]), whereas some kinetic effect can be recorded at pH 3.0 and 0.001M NaCl ($PdCl_2(aq)$/PdOHCl(aq)/$Pd(OH)_2(aq)$/$PdCl^+$ possible species [5]) (Figure S8). $PdCl_4^{2-}$ and $Pd(H_2O)Cl_3^-$ species are repelled by the negative micellar surface and cannot reach the ligand strongly buried inside the micelle, whereas other non-negative species do. Taken altogether these data confirm a picture where the binding of the PdP^{4+} complex to negative substrates as SDS and DNA is strong and driven by both electrostatic and hydrophobic forces.

Conclusions The kinetic analysis of $PdCl_4^{2-}$ binding to 5,10,15,20-tetrakis(1-methyl-4-pyridiyl)-porphyne (H_2P^{4+}) has shown that the planar complex can be formed in NaCl water solution by simple mixing of the reagents. No sitting-atop geometries are evidenced. The binding is quantitative for $T \leq 40°C$ and undergoes completion in some hours. The low complexation rates agree with the rigidity of the ring and with the energy penalty to be paid for H^+ and Cl^- expulsion. The activation thermodynamic parameters for complex formation were evaluated by

temperature dependence of the rate constants and agree with a palladium complexation mechanism that goes through an associative SN_2IP step. As for DNA binding, the thermodynamic and kinetic study indicate that the planar Pd(II)-complex strongly (higher affinity with respect to similar M(II)P^{4+} complexes [35,39]) and fully intercalates between base pairs, producing a significant distortion of DNA. In the final structure, PdP^{4+} is totally protected from the outer environment, grace to the synergistic effect of base-dye interaction (hypochromic and bathochromic effects), electrostatic attraction, hydrophobic forces. According to a slow process, DNA can better accommodate the intercalator or even covalent binding of the Pd(II) ion to the nucleobase might occur. The presence and type of metal ion play a crucial role, as blank tests performed with H_2P^{4+} or CuP^{4+} demonstrate that these species show lower affinity to the DNA helix.

Experimental

Materials Sigma-Aldrich provided the 5,10,15,20-tetrakis(1-methyl-4-pyridyl)21H,23H-porphyrin tetra-p-tosylate (H_2P^{4+}) salt (purity > 97%). Concentrations of porphyrin ligand (obtained by dissolving known amounts of solid in water) are expressed as C_L. Palladium(II), in the form of 1.6×10^{-3} M H_2PdCl_4 water solution, was a kind gift from CHIMET s.p.a. Copper(II) was the $Cu(NO_3)_2\cdot 3H_2O$ salt from Sigma-Aldrich, its solutions

are prepared by dissolving known amounts of solid in water. Concentrations of palladium or copper ions are expressed as C_M.

Calf thymus DNA (lyophilised sodium salt, highly polymerised) from Sigma-Aldrich was dissolved into water and sonicated producing short polynucleotide fragments (ca. 300 base pairs) according to a known procedure [14]. Stock solutions of DNA were standardised spectrophotometrically (ε = 13200 $M^{-1}cm^{-1}$ at 260 nm, I = 0.10 M, pH = 7.0 [17]); concentrations of DNA are expressed in molarity of base pairs and indicated as C_P. In the Pd(II)-porphyrin/DNA studies, the pre-formed 1:1 complex (interacting dye) concentration will be indicated as C_D. Sodium-dodecyl-sulphate (SDS) was from Sigma-Aldrich, known amounts of solid were dissolved into water to obtain 0.2 M stock solutions. Dodecyl trimethyl ammonium chloride (DTAC), from Fluka, was also dissolved into water to obtain 0.2 M stock solutions. The working solution are well above the critical micellar concentration [16,18]. Chemicals not expressly cited are of analytical grade and were used without further purification. All solutions, in particular of porphyrin and DNA, were freshly prepared and kept at 4 °C in the dark. The water used to prepare the solutions and as a reaction medium was ultra-pure 18.2 MΩ water from a Sartorius purification system.

Methods Measurements of pH were made by a Metrohm 713 pH-meter equipped with a combined glass electrode. A Shimadzu UV-2450 spectrophotometer was used to record absorption spectra and to perform spectrophotometric titrations whereas a PerkinElmer LS55 spectrofluorometer is used for fluorescence measurements. Both apparatuses are equipped with jacketed cell holders, and allow temperature control to within ±0.1°C. The Pd(II)-porphyrin complex/DNA titrations were carried out by adding increasing amounts of DNA directly into the cell containing the complex solution, whose initial concentration was in the range 2.0-2.5×10^{-6} M. The additions were made by a Hamilton micro syringe connected to a Mitutoyo micrometric screw; this system enables additions as small as 0.166 μL. Absorbance titrations were analysed at λ = 417 nm, fluorescence titrations at λ_{ex} = 500 nm and λ_{em} = 572 nm.

Kinetics of Pd(II)-porphyrin complex formation was analysed at pH 3.0 by measuring absorbance changes in time at NaCl 0.2 M and 422 nm for C_L = 9.6×10^{-7} M and 8.26×10^{-5} M < C_M < 7.05×10^{-4} M (C_M >> C_L). The rate of this reaction is slow, so that the kinetic traces were recorded by the spectrophotometer. Blank test were also performed that showed that absorbance change/bleaching of porphyrin alone was negligible. Nevertheless, kinetic traces are differential curves, i.e. the reference cell contained the same amount of the porphyrin ligand alone, whereas

measuring cell contained the ligand+metal mixture. The temperature was kept constant using a thermostat (± 0.1°C), the exact value of temperature inside the cell was periodically checked using a micro-thermometer. Other two series of experiments were devised as follows: (A) $C_L = 9.6\times10^{-7}$ M, $C_M = 4.00\times10^{-4}$ and different [Cl^-] and ionic strength (I); (B) $C_L = 9.6\times10^{-7}$ M, $C_M = 4.00\times10^{-4}$, different [Cl^-] but constant I = 0.2 M (obtained by suitable addition of $NaClO_4$).

The kinetic measurements on the Pd(II)-porphyrin complex interaction with DNA (NaCl 1.0 M, 40 °C) were performed using a T-jump apparatus assembled in our laboratory [14]. In the present study absorbance changes at λ = 420 nm were monitored. Relaxation times were measured for a range of DNA concentrations under the conditions $C_D = 5.0\times10^{-6}$ M, $C_P = 5.0\times10^{-6} \div 3.87\times10^{-5}$ M. Each experiment was repeated at least six times, and the observed spread of time constants was found to be within 10%. The time constants given in this work are average values.

Viscosity measurements were performed using a Micro-Ubbelohde viscometer whose temperature was controlled by an external thermostat (25 ± 0.1 ºC). Time of flow is measured by a digital stopwatch; the data used for each sample are the average of five repeated experiments (error within 5%).

The partitioning of the porphyrin between micelles and water has been determined using a combination of spectrophotometric and ultrafiltration methods already described [18]. In this work, the experiments were done on mixtures that contain 3.0×10^{-6} M H_2P^{4+} and 0.03 M SDS or DTAC.

ACKNOWELDGEMENTS: The financial support by PRA 2017 of the University of Pisa - project PRA_2017_28, from "la Caixa" Foundation (project OSLC-2012-007), MINECO - Spain (CTQ2014-58812-C2-2-R, FEDER Funds) and Junta de Castilla y León (BU042U16, FEDER Funds) is gratefully acknowledged.

References

1. Sun RWY, Li CKL, Ma DL, Yan JJ, Lok CN, Leung CH, Zhu NY, Che CM (2010) Chem - Eur J 16:3097.
2. Cao Q, Li Y, Freisinger E, Qin PZ, Sigel RKO, Mao ZW Inorg Chem Front 4:10.
3. Singh S, Aggarwal A, Bhupathiraju NVSDK, Arianna G, Tiwari K, Drain CM (2015) Chem Rev 115:10261.
4. Rury AS, Wiley TE, Sension RJ (2015) Acc Chem Res 48:860.
5. Shi L-M, Pan J-X, Zhou B, Jiang X (2015) J Mater Chem B 3:9340.
6. Lalaoui N, Le Goff A, Holzinger M, Cosnier S (2015) Chem - Eur J 21:16868.
7. Liu SF, Moh LCH, Swager TM (2015) Chem Mater 27:3560.
8. Koifman OI, Ageeva TA (2014) Polym Sci Ser C+ 56:84.
9. Ning X, Ma L, Zhang S, Qin D, Shan D, Hu Y, Lu X (2016) J Phys Chem C 120:919.
10. Sato T, Mori W, Kato CN, Yanaoka E, Kuribayashi T, Ohtera R, Shiraishi Y (2005) J Catal 232:186.
11. Kostas ID, Coutsolelos AG, Charalambidis G, Skondra A (2007) Tetrahedron Lett 48:6688.
12. Amir MK, Khan SZ, Hayat F, Hassan A, Butler IS, Zia-ur-Rehman. (2016) Inorg Chim Acta 451:31.

13. Bakalova AG (2013) Curr Trends Med Chem 7:53.

14. Tsekova D, Gorolomova P, Gochev G, Skumryev V, Momekov G, Momekova D, Gencheva G (2013) J Inorg Biochem 124:54.

15. Guo L, Dong W, Tong X, Dong C, Shuang S (2006) Talanta 70:630.

16. Gibbs EJ, Maurer MC, Zhang JH, Reiff WM, Hill DT, Malicka-Blaszkiewicz M, McKinnie RE, Liu H-Q, Pasternack RF (1988) J Inorg Biochem 32:39.

17. Pasternack RF, Sutin N, Turner DH (1976) J Am Chem Soc 98:1908.

18. Pasternack RF, Antebi A, Ehrlich B, Sidney D, Gibbs EJ, Bassner SL, Depoy LM (1984) J Mol Cat 23:235.

19. Kadish KM, Maiya BG, Araullo-McAdams C (1991) J Phys Chem 95:427.

20. Xu X, Zhang H, Zhang C, Cheng J (1991) Anal Chem 63:2529.

21. High LRH, Holder SJ, Penfold HV (2007) Macromolecules (Washington, DC, U. S.) 40:7157.

22. Choi E-Y, Barron PM, Novotny RW, Son H-T, Hu C, Choe W (2009) Inorg Chem 48:426.

23. Milot RL, Moore GF, Crabtree RH, Brudvig GW, Schmuttenmaer CA (2013) J Phys Chem C 117:21662.

24. Lomova TN, Klyueva ME, Tyulyaeva EY, Bichan NG (2012) J Porphyrins Phthalocyanines 16:1040.
25. Baes CF, Mesmer RE (1976) The hydrolysis of cations. Wiley
26. Valicsek Z, Eller G, Horvath O (2012) Dalton Trans 41:13120.
27. Lawrence MAW, Jackson YA, Mulder WH, Bjoeremark PM, Hakansson M (2015) Aust J Chem 68:731.
28. Chosh PK, Saha S, Mahapatra A (2009) Int J Chem Kinet 41:463.
29. Chaires JB (2006) Arch Biochem Biophys 453:26.
30. Biver T, Lombardi D, Secco F, Tine MR, Venturini M, Bencini A, Bianchi A, Valtancoli B (2006) Dalton Trans 1524.
31. Biver T, Secco F, Tine MR, Venturini M, Bencini A, Bianchi A, Giorgi C (2004) J Inorg Biochem 98:1531.
32. Bernges F, Holler E (1991) Nucleic Acids Res 19:1483.
33. Biver T (2013) Coordin Chem Rev 257:2765.
34. Meiser C, Song B, Freisinger E, Peilert M, Sigel H, Lippert B (1997) Chem - Eur J 3:388.
35. Aydinoglu S, Biver T, Secco F, Venturini M (2010) Int J Chem Kinet 42:79.
36. Aydinoglu S, Biver T, Secco F, Venturini M (2014) Colloid Surf A 461:303.
37. Felsenfeld G, Hirschman SZ (1965) J Mol Biol 13:407.

38. Biver T, Boggioni A, Secco F, Venturini M (2008) Langmuir 24:36.

39. Pasternack RF, Gibbs EJ, Villafranca JJ (1983) Biochemistry 22:5409.

Figure Captions

Fig. 1. Molecular formula of 5,10,15,20-tetrakis(1-methyl-4-pyridiyl)-porphyne in its unprotonated form (H_2P^{4+}).

Fig. 2. A) UV-vis spectra in water of 9.6×10^{-7} M H_2P^{4+} (▬) and of 9.6×10^{-7} M H_2P^{4+} + 7.05×10^{-4} M $PdCl_4^{2-}$ (- • -); B) absorbance difference (see Methods section) variation in time at λ = 422 nm monitoring PdP^{4+} complex formation for 9.6×10^{-7} M H_2P^{4+} + 7.05×10^{-4} M $PdCl_4^{2-}$, the dotted line is the mono-exponential fit. For both A) and B) $[H^+] = 10^{-3}$ M, I = 0.2 M (NaCl), T = 25°C.

Fig. 3. Time constant ($1/\tau$) dependence on the palladium content ($C_M >> C_L$) for the formation of PdP^{4+} metal complex; $C_L = 9.6\times10^{-7}$ M, $[H^+] = 10^{-3}$ M, I = 0.2 M (NaCl), T = 25 °C (●), 40 °C (■), 55 °C (▲) and 65 °C (○).

Fig. 4. Time constant ($1/\tau$) dependence on the medium for the formation of PdP^{4+} metal complex; $C_L = 9.6\times10^{-7}$ M, $C_M = 4.0\times10^{-4}$ M, $[H^+] = 10^{-3}$ M, T = 40 °C; (●) different [NaCl] and thus different total salt content; (■) experiments at I = 0.2 M = [NaCl] + [$NaClO_4$].

Fig. 5. (A) Absorbance spectra variation for PdP^{4+} upon addition of increasing amounts of DNA and (B) relevant binding isotherm at 417 nm; C_D = 2.0 μM, C_P = 0 to 38 μM, pH 7.0, NaCl 1.0 M, NaCac 0.01 M, T = 25.0°C.

Fig. 6. Van't hoff plot for the PdP^{4+}/DNA system; ■ spectrophotometric titrations, ○ spectrofluorometric titrations, ★ kinetics ($K^{DNA} = k_f^{DNA}/k_d^{DNA}$), pH 7.0, NaCl 1.0 M, NaCac 0.01 M.

Fig. 7. Binding isotherm for PdP^{4+}/DNA fluorescence titration and relevant analysis according to Eq. (5) (inset); C_D = 2.5 μM, C_P = 0 to 22 μM, λ_{ex} = 500 nm, λ_{em} = 572 nm, pH 7.0, NaCl 1.0 M, NaCac 0.01 M, *T* = 25.0°C.

Fig. 8. Kinetic analysis (T-jump technique) of PdP^{4+}/DNA binding: A) example of relaxation curve (C_P = 38.7 μM, λ = 420 nm) and B) reciprocal relaxation time dependence on reactant concentrations (C_P = 5.0 to 38.7 μM); C_D = 2.0 μM, pH 7.0, NaCl 1.0 M, NaCac 0.01 M, *T* = 40.0°C.

Fig. 9. Stern-Volmer plot for the quenching by iodide of PdP^{4+} (open mark) and PdP^{4+}/DNA (full mark); C_D = 1.9 μM, C_P = 24.9 μM, λ_{ex} = 470 nm, λ_{em} = 555 nm, pH 7.0, *T* = 25.0°C.

Fig. 10. Relative viscosity $(\eta/\eta°)^{1/3}$ dependence on the dye/DNA ratio for different porphyrin/DNA systems: (□) PdP^{4+}, (●) CuP^{4+} (▲) and H_2P^{4+}; C_P = 2.79×10^{-4} M, NaCl 0.1 M, pH 7.0, *T* = 25.0°C.

Fig. 11. Percentage of absorbance variation (100*|A(t)-A(0)|/A(0)) recorded in time for the PdP^{4+}/DNA system at different wavelengths; C_D = 1.77×10^{-5} M, C_P = 1.81×10^{-4} M, I = 1.0 M, pH = 7.0, *T* = 25.0 °C, total time = 186 min; (Δ) 415 nm, (▲) 439 nm, (○) 522 nm, (●) 542 nm.

Table 1. Apparent kinetic parameters for PdP^{4+} complex formation; I = 0.2 M (NaCl), pH = 3. *Data in italics* are rough estimates, based on the non-distinguishable from zero intercepts of the plots in Figure 3.

T **/°C**	25	40	55	65
$\mathbf{k_f^{app}}$ **/M^{-1} s^{-1}**	0.19	0.47	1.21	2.14
$\mathbf{k_d^{app}}$ **/s^{-1}**	*< 2.0×10^{-6}*	*< 1.0×10^{-5}*	2.46×10^{-4}	6.99×10^{-4}
$\mathbf{K_{app}}$ **/M^{-1}** [a]	*> 9.5×10^{4}*	*> 4.7×10^{4}*	4.92×10^{3}	3.06×10^{3}

[a] $K_{app} = k_f^{app}/k_d^{app}$

Figure 1

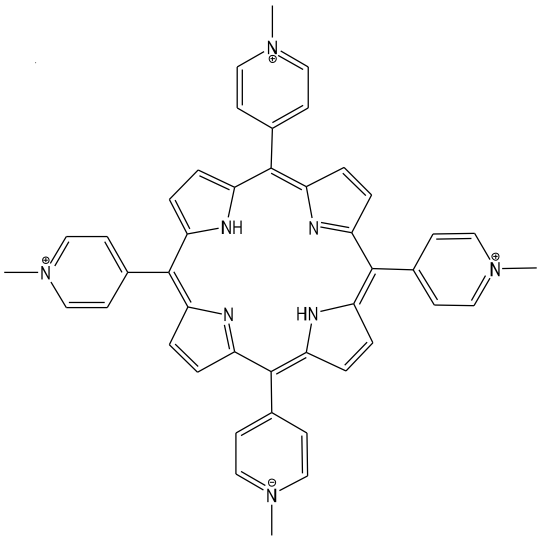

Figure 2

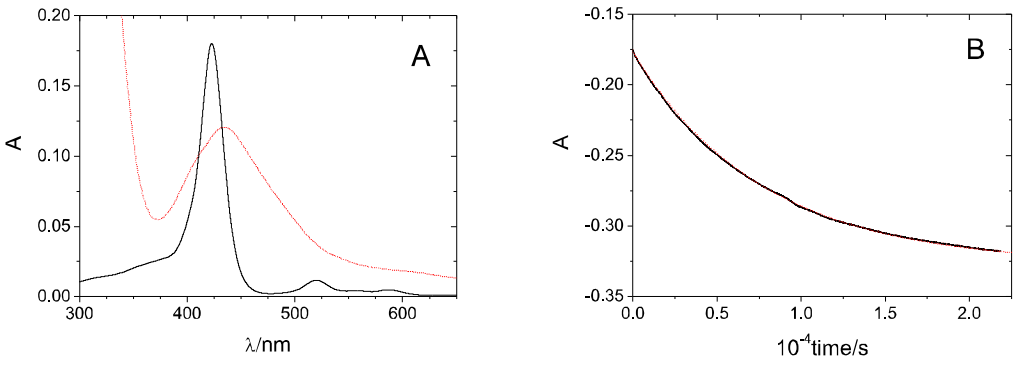

Figure 3

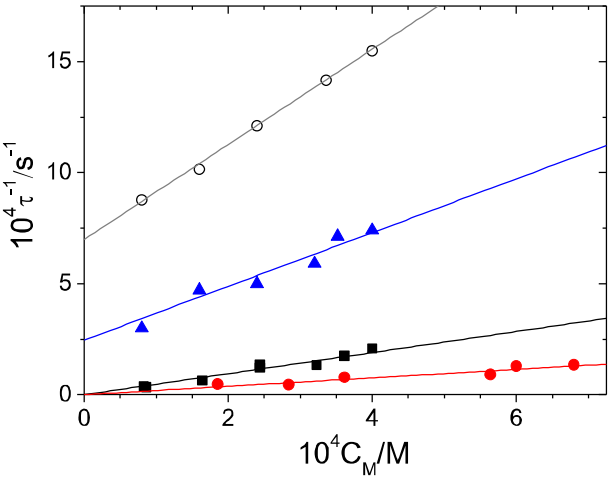

Figure 4

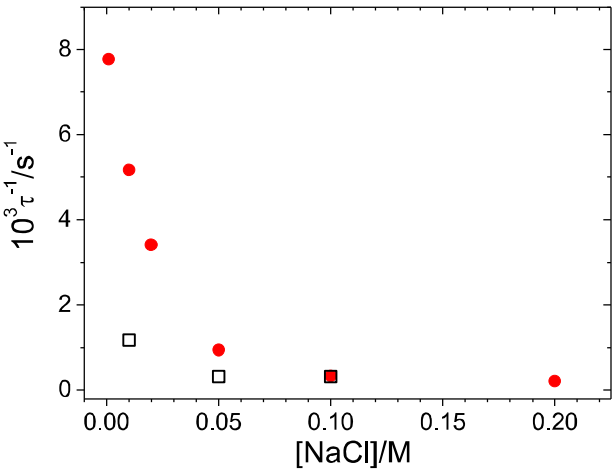

Figure 5

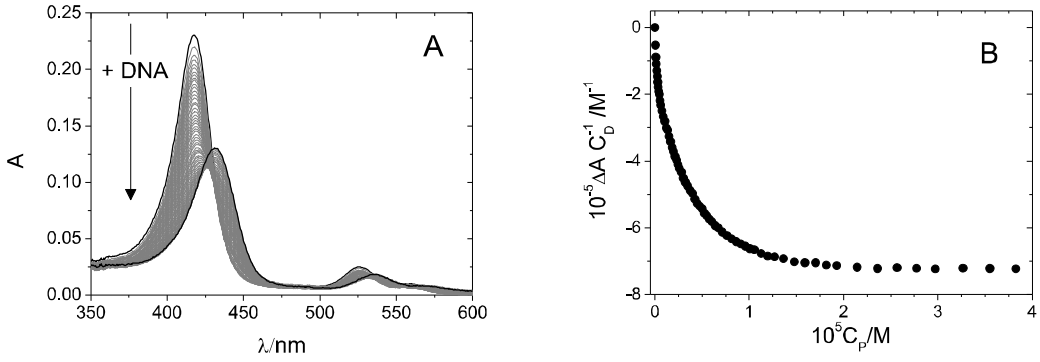

Figure 6

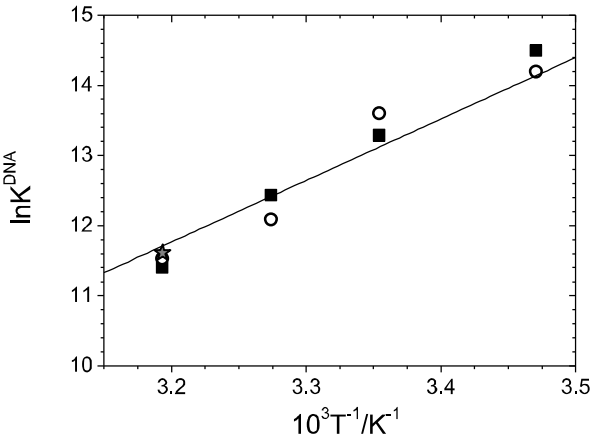

Figure 7

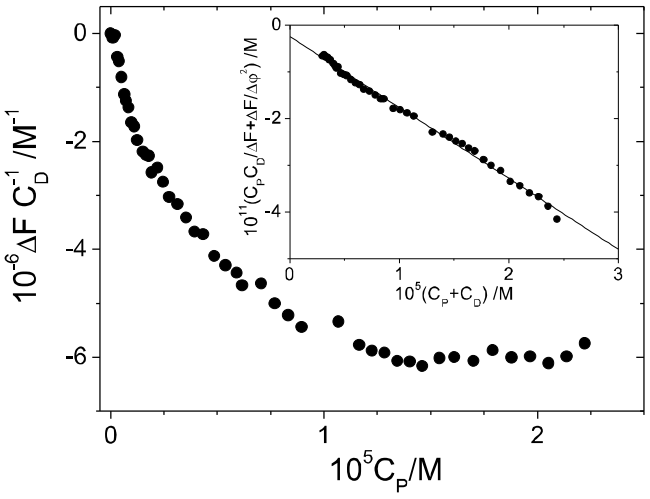

Figure 8

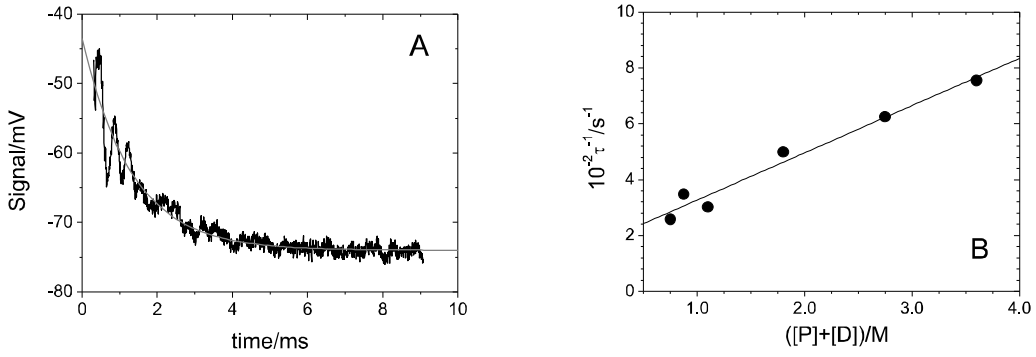

Figure 9

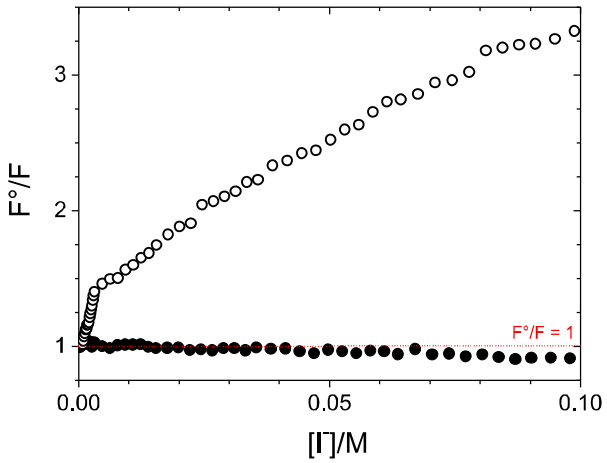

Figure 10

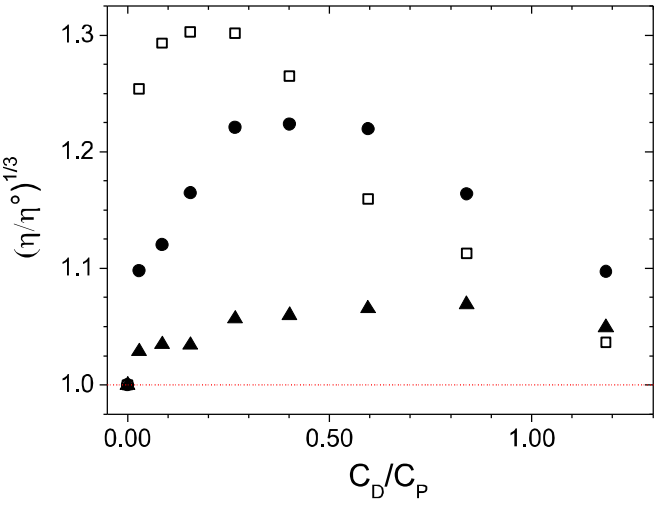

Figure 11

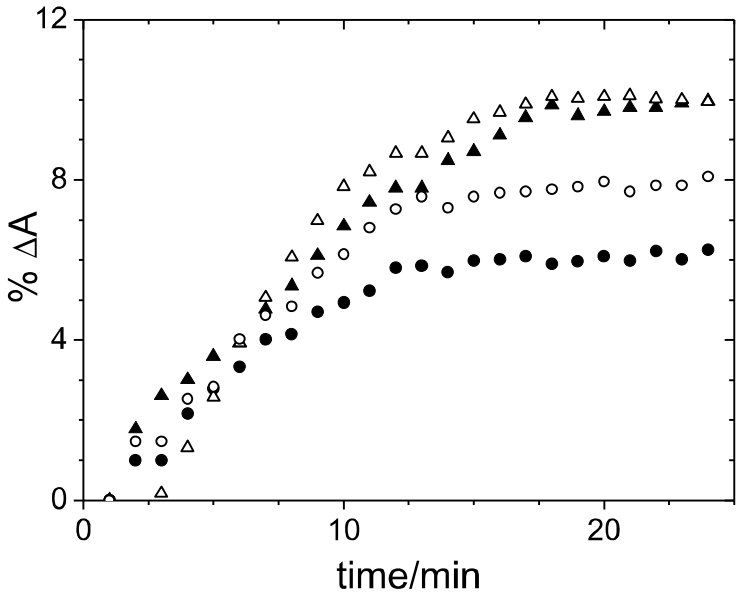

1 Graphical abstract

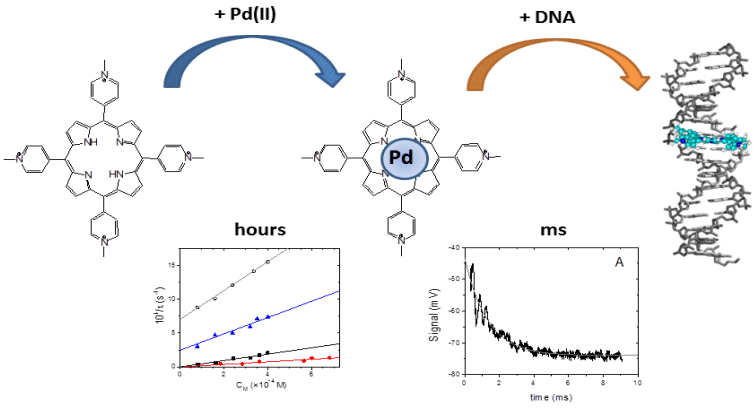

2